

# Modeling and Control of Multi-Contact Centers of Pressure and Internal Forces in Humanoid Robots

Luis Sentis, Jaeheung Park, and Oussama Khatib

**Abstract**—This paper presents a methodology for the modeling and control of internal forces and moments produced during multi-contact interactions between humanoid robots and the environment. The approach is based on the virtual linkage model which provides a physical representation of the internal forces and moments acting between the various contacts. The forces acting at the contacts are decomposed into internal and resulting forces and the latter are represented at the robot's center of mass. A grasp/contact matrix describing the complex interactions between contact forces and center of mass behavior is developed. Based on this model, a new torque-based approach for the control of internal forces is suggested and illustrated on the Asimo humanoid robot. The new controller is integrated into the framework for whole-body prioritized multitasking enabling the unified control of operational tasks, postures, and internal forces.

## I. INTRODUCTION

An important problem in humanoids is their ability to manipulate and maneuver in their environments through compliant multi-contact interactions. This ability is a necessary step toward enabling humanoids to operate skillfully and safely in highly constrained environments. To address this challenge, we propose here models describing the complex dependencies between whole-body contacts and we analyze their control and integration with functional behaviors. We create contact representations using the virtual linkage model [23] describing the relationship between reaction forces on contact bodies with respect to resultant forces at the robot's center of mass, pressure points, and internal tensions between contact closed loops. We investigate the dynamics of closed loops and exploit the virtual linkage model to develop a controller that guides internal force behavior between contact nodes. We integrate the proposed control method with our framework for prioritized multitasking [21], addressing the unified control of constraints, balance, tasks, postures, and multi-contact behavior. This work is done as part of the Honda Asimo project at Stanford, which implements a torque-based control framework for a research version of the Asimo robot.

Contact interactions in robots have been addressed since the early 1980s with work on dynamics and force control in the context of robotic manipulation [10] [17]. Cooperative distributed manipulation became important to enable the handling of heavy or big objects [1]. To describe the behavior of the object independently of the manipulators, an augmented object model was proposed based on dynamically consistent models [11]. Research began to focus on modeling multi-grasp behaviors and the associated internal forces acting between manipulators [14]. Using a closed-chain mechanism called the virtual linkage model, decoupled object behavior and accurate dynamic control of internal forces was addressed [23]. Mobile robotic platforms equipped with robotic manipulators were developed [8] and multi-grasp manipulation was implemented using efficient operational

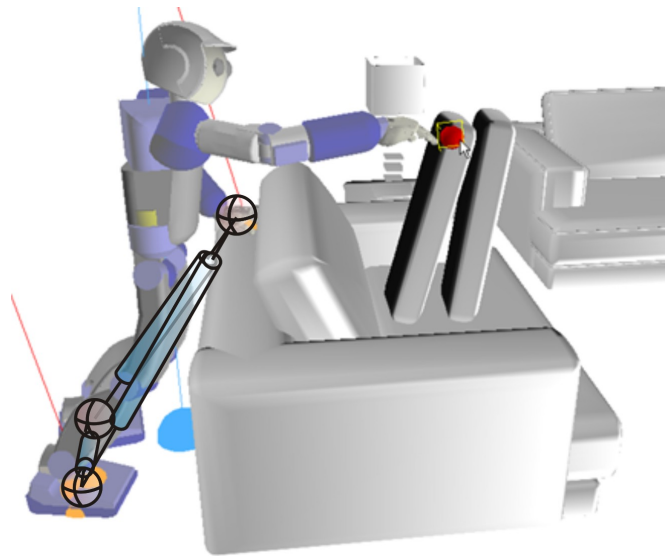


Fig. 1. Realtime simulation of a multi-contact behavior with user-enabled interactive control of the robot's right hand. A virtual linkage model is overlaid capturing the internal force behaviors acting between supporting bodies.

space algorithms [2]. The dynamics and control of task and postural behaviors in humanoid robots were addressed and prioritized multitask controllers were developed to enable the unified force-level control of constraints, task, and postures [20].

The aim of this new research is to analyze and model whole-body multi-contact interactions and provide a control platform that enables humanoids to manipulate and maneuver efficiently in their environments. It is therefore important to understand the relationship between reaction forces on contact bodies, internal tensions and moments acting between these contacts, and whole-body task and motion behaviors. Because this work connects with legged locomotion, it is useful to review modern developments on this area of research. Dynamic legged locomotion has been a center of attention since the 1960s [4]. The Zero Moment Point criterion (ZMP) was developed to evaluate center of mass (CoM) acceleration boundaries [22]. Implementations of simple dynamic control algorithms for multi-legged running robots followed [16]. ZMP methods for humanoid robots were pioneered with the development of the Honda humanoid program [7]. To enable generalized multi-contact locomotion behaviors, extensions to the ZMP dynamic evaluation criterion were developed [6]. Recently, a force level balancing controller based on minimum norm distribution of contact forces has been developed [9].

In this paper, we analyze and control the interactions between whole-body contacts, balance, and task behaviors.

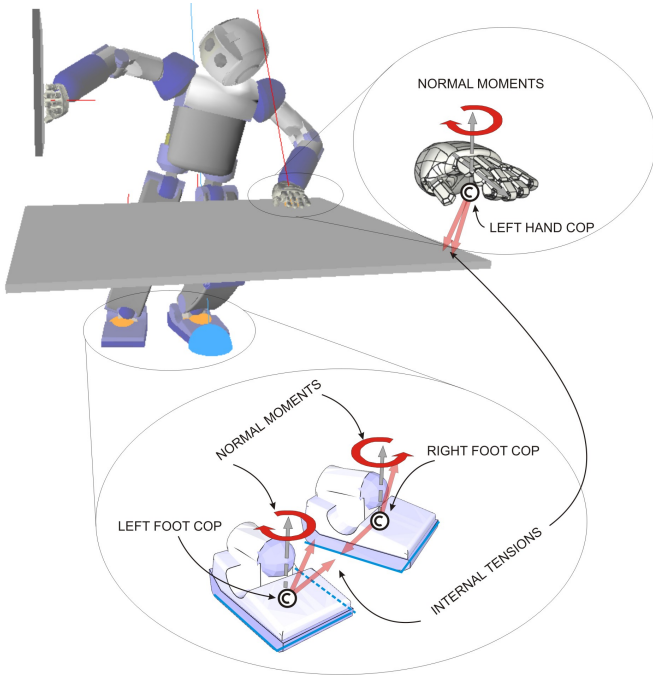


Fig. 2. **Decomposition of internal forces and moments:** We decompose internal forces and moments into contact centers of pressure, internal tensions, and normal moments. Contact centers of pressure allow us to control the behavior contact rotational constraints while internal tensions and normal moments allow us to control the behavior of contact points with respect to surface friction properties.

We define multiple centers of pressure (CoP's) to abstract the behavior of contact bodies. When the center of pressure of a contact body approaches an edge, a non zero moment takes place about that edge causing the body to rotate. By controlling the position of contact centers of pressure we control the behavior of contact rotational conditions. We use the virtual linkage model to describe multi-contact whole-body behaviors as well as CoM behavior. We define a grasp/contact matrix to establish the relationship between resultant forces at the CoM, and internal and reaction forces on contact bodies. We create dynamically correct controllers to govern the behavior of contact CoP's, internal tensions and normal moments. Using control structures that are orthogonal to CoM and task behavior, we integrate internal force controllers with our previous framework for prioritized multitask control.

The capabilities and effectiveness of our methods are validated through whole-body multi-contact scenarios simulated on a dynamical simulator of the Honda Asimo robot. CoM tracking, fulfillment of contact constraints, and internal force control are achieved with high accuracy.

## II. MODELING OF CONTACT COP'S AND INTERNAL FORCES USING THE VIRTUAL LINKAGE MODEL

We consider whole-body contact scenarios with surface to surface contacts, where multiple extremities of the robot are in static contact against flat surfaces (see Figure 2). In this case, every contact imposes six constraints on the robot's mobility. We assume each extremity in contact has enough degrees of freedom with respect to the base link to control independently its position and orientation. Flat supporting contacts impose  $6 \times n_s$  constraints on the motion, where 6 of these constraints provide the support to manipulate the robot's base and the other  $6 \times (n_s - 1)$  describe the internal

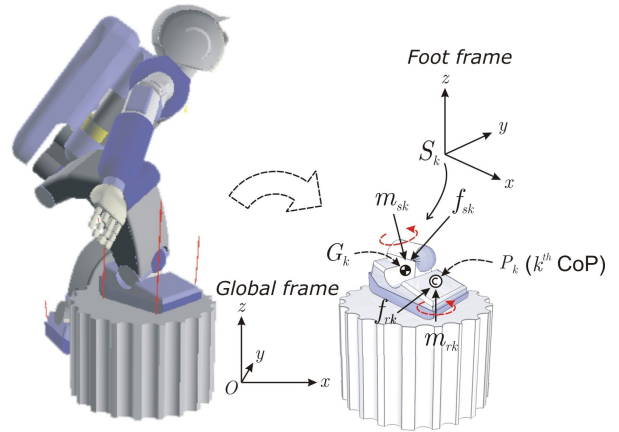


Fig. 3. Forces acting on the  $k^{th}$  supporting body (e.g. the right foot): Establishing the balance of moments on each contact body allows us to determine the position of contact centers of pressure.

forces and moments acting on the closed loops between supporting extremities [23]. Here,  $n_s$  represents the number of extremities in contact. Internal forces and moments play two different roles in characterizing the contact behavior of the robot: (1) Contact centers of pressure define the behavior of the contacts with respect to edge or point rotations. (2) Internal tensions and moments describe the behavior of the contacts with respect to the friction characteristics associated with the contact surfaces.

For  $n_s$  links in contact we associate  $n_s$  contact CoP's. Each contact center of pressure is defined as the 2D point on the contact surface where resultant tangential moments are equal to zero. Therefore,  $2 \times n_s$  coordinates describe all contact pressure points. In Figure 2 we illustrate a contact scenario with all contact forces and moments acting on supporting extremities. We focus on the forces and moments taking place on a particular contact body (see Figure 3). Based on [22], we neglect the body above the  $k^{th}$  supporting extremity and replace its influence by the inertial and gravitational force and moment  $f_{s_k}$  and  $m_{s_k}$  acting on the foot's sensor point  $S_k$ . Here,  $P_k$  is the foot's center of pressure,  $f_{r_k}$  is the reaction force acting on  $P_k$ , and  $m_{r_k}$  is the reaction moments acting on  $P_k$ . The frame  $\{O\}$  represents an inertial frame of reference located outside of the robot and the frame  $\{S_k\}$  represents a frame of reference located at the sensor point. All force quantities are described with respect to the sensor frame. Assuming the supporting foot is in static equilibrium, we formulate the following balance equation between inertial, gravitational, and reaction moments [5],

$$OP_k \times f_{r_k} + m_{r_k} = OS_k \times f_{s_k} + m_{s_k} - OG_k \times M_k g. \quad (1)$$

Here,  $G_k$  is the center of gravity of the  $k^{th}$  supporting extremity,  $M_k$  is the mass below the sensor point and  $g$  is the gravitational acceleration vector. To compute the foot's centers of pressure we consider the tangential part of the above equation with respect to the contact surface, i.e.

$$\left[ OP_k \times f_{r_k} = OS_k \times (f_{s_k} - M_k g) + m'_{s_k} \right]_{\mathcal{T}_k}. \quad (2)$$

where

$$m'_{s_k} \triangleq m_{s_k} - S_k G_k \times M_k g \quad (3)$$

is a modified moment that includes the moment arm of the gravity at the sensor point, the superscript  $\mathcal{T}_k$  denotes

tangential directions of the  $k^{th}$  contact body. Note that  $m_{r_k}$  does not appear above because the definition of contact CoP implies zero tangential moments. Considering the force balance equation

$$f_{r_k} = f_{s_k} - M_k g, \quad (4)$$

we arrange Equation (2) as

$$\left[ (OP_k - OS_k) \times f_{r_k} \right]^{T_k} = m'_{s_k} T_k, \quad (5)$$

and solve it to get the center of pressure for the  $k^{th}$  contact link:

$$P_{kx} = S_{kx} - \frac{f_{r_{kx}}}{f_{r_{kz}}} (S_{kz} - P_{kz}) - \frac{m'_{sy}}{f_{r_{kz}}}, \quad (6)$$

$$P_{ky} = S_{ky} - \frac{f_{r_{ky}}}{f_{r_{kz}}} (S_{kz} - P_{kz}) + \frac{m'_{sx}}{f_{r_{kz}}}. \quad (7)$$

Here,  $x$  and  $y$  refer to the tangential directions with respect to the local surface frames. The same analysis applies to the other extremities in contact, defining the  $n_s$  contact centers of pressure.

To further characterize contact CoP's, we formulate the relationship between resultant moments at contact CoP's and reaction forces on contact bodies:

$$m_{\text{cop}} \triangleq \begin{pmatrix} [m_{r1}]^{T_1} \\ \vdots \\ [m_{rn_s}]^{T_{n_s}} \end{pmatrix} = S_{\text{cop}} T_{\text{cop}} F_r = 0 \quad \epsilon \mathcal{R}^{2n_s}, \quad (8)$$

where  $F_r$  is the vector of reaction forces and moments expressed with respect to the location of contact CoP's in global frame, i.e.

$$F_r \triangleq \begin{pmatrix} f_{r1} \\ \vdots \\ f_{rn_s} \\ m_{r1} \\ \vdots \\ m_{rn_s} \end{pmatrix} \epsilon \mathcal{R}^{6n_s}, \quad (9)$$

$m_{\text{cop}}$  is the vector of tangential moments at contact CoP locations expressed in local frames,  $m_{r_k}$  is the  $k^{th}$  component of resultant moments,  $T_{\text{cop}}$  is a matrix that translates and rotates forces and moments from global frame to local surface frames, and  $S_{\text{cop}}$  is a selection matrix that selects tangential moments. Notice that in Equation (8) CoP conditions are modeled as zero tangential moments.

Based on these models, we will develop methods for the efficient control of the internal contact state of the robot, while fulfilling dynamic stability constraints. In particular, we will present control methods that allow us to manipulate contact CoP's to desired locations on the contact surfaces. By manipulating contact CoP's away from contact edges we ensure that contact surfaces stay flat against the supporting surfaces avoiding undesired contact rotations. Additionally, controlling contact CoP's will result in compliant contact behaviors since they imply neutralizing tangential moments exerted by contact surfaces. The various properties of contact CoP's make them an effective abstraction for the control and analysis of contact rotational behaviors.

We focus on the characterization of internal force behavior between closed loops formed by the contact extremities. We introduce a new instance of the virtual linkage model [23] to describe the complex contact dependencies associated with the closed loops. The virtual linkage model is a parallel multi-DoF mechanical system connecting contact nodes via virtual prismatic and spherical joints. It was first introduced to describe the relationship between resultant and internal forces of a shared object between multiple manipulators. In the case of humanoids, the extremities in contact play the role of the manipulators and the terrain is the object of interaction.

We associate a virtual linkage model connecting contact extremities with nodes anchored at center of pressure locations and prismatic joints attached to the nodes. As shown in Figure 4 each extremity in contact introduces a tension with respect to other nodes as well as normal and tangential moments with respect to the contact surfaces. For contacts with  $n_s > 2$  we can independently specify  $3 \times (n_s - 2)$  tensions,  $n_s$  normal moments, and  $2 \times n_s$  tangential moments describing contact centers of pressure. When  $n_s = 2$  we can specify one tension force, and five tangential and normal moments. The details of this case will be described in the journal version of this paper. Any additional extremity in contact will introduce three new tensions with respect to other nodes, and three more moments with respect to the surface contact. No more than three tensions per node with respect to other nodes can be independently specified. Internal tensions characterize the behavior of contact bodies with respect to the friction cones of the surfaces in contact while normal moments characterize the fulfillment of unilateral contact conditions. The relationship between tension and reaction forces can be formulated as

$$f_t \triangleq \begin{pmatrix} \vdots \\ f_{tij} \\ \vdots \end{pmatrix} = S_t R_t \Delta_t F_r \quad \epsilon \mathcal{R}^{3(n_s-2)}, \quad (10)$$

where  $ij$  are pairs of nodes,  $\Delta_t$  is a differential matrix operator that subtracts pairs of forces between contact nodes,  $R_t$  is a cumulative rotation matrix from global frame to the directions linking virtual linkage nodes, and  $S_t$  is a selection matrix choosing tension directions. Similarly, we characterize normal moments as

$$m_n \triangleq \begin{pmatrix} m_{n1} \\ m_{n2} \\ \vdots \\ m_{nn_s} \end{pmatrix} = S_n T_s F_r \quad \epsilon \mathcal{R}^{n_s}, \quad (11)$$

where  $T_s$  is a cumulative rotation matrix rotating quantities from global frame to surface frames, and  $S_n$  is a selection matrix choosing normal directions.

To complete the virtual linkage model, we establish the relationship between resultant and internal forces and moments acting at the robot's center of mass. The robot's center of mass is an important abstraction for analysis and control because it characterizes the maneuverability of the robot to plan locomotion behaviors. Similarly to the relationships developed in the original virtual linkage model [23], we formulate the equations describing the balance of reaction forces and moments at contact bodies with respect to the resultant forces and moments taking place at the

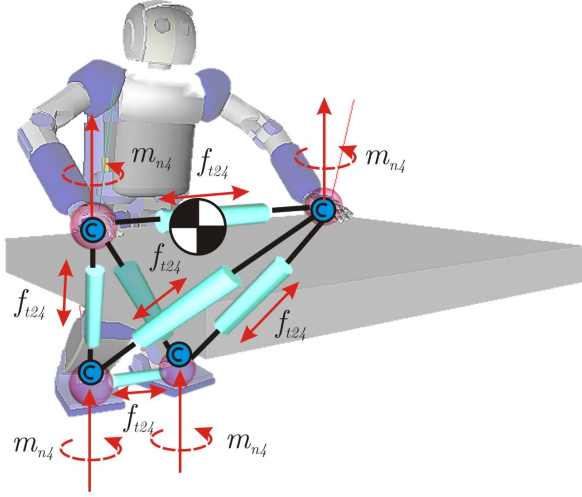


Fig. 4. Virtual linkage model for humanoid robots: We define a virtual linkage model uniting contact CoP's, enabling the characterization of internal tensions between nodes and normal moments against contact surfaces. Tangential moments are implicitly characterized through CoP positions. The virtual linkage model also addresses the behavior of contact forces with respect to CoM behavior.

robot's center of mass:

$$\begin{pmatrix} [I]_{3 \times 3} & \cdots & [I]_{3 \times 3} & | & [0]_{3 \times 3} & \cdots & [0]_{3 \times 3} \\ \hat{P}_1 & \cdots & \hat{P}_n & | & [I]_{3 \times 3} & \cdots & [I]_{3 \times 3} \end{pmatrix} F_r = \begin{pmatrix} [I]_{3 \times 3} & | & [0]_{3 \times 3} \\ \hat{P}_{\text{com}} & | & [I]_{3 \times 3} \end{pmatrix} F_{\text{com}}, \quad (12)$$

where  $[\cdot]$  indicates the cross product operator,  $P_i$  is the position of the  $i^{\text{th}}$  contact CoP,  $P_{\text{com}}$  is the position of the center of mass, and  $F_{\text{com}}$  is the six dimensional vector of inertial and gravitational forces and moments at the robot's center of mass. Combining (8), (10), (11), and (12) we obtain the following virtual linkage model for humanoid robots

$$\begin{pmatrix} F_{\text{com}} \\ F_{\text{int}} \end{pmatrix} = G F_r \quad (13)$$

where  $F_{\text{int}}$  is the vector of internal forces and moments defined as

$$F_{\text{int}} \triangleq \begin{pmatrix} f_t \\ m_{\text{cop}} \\ m_n \end{pmatrix} \in \mathcal{R}^{6(n_s-1)}, \quad (14)$$

and  $G$  is a grasp/contact matrix [23] defined as

$$G \triangleq \begin{pmatrix} W_{\text{com}} \\ W_{\text{int}} \end{pmatrix} \in \mathcal{R}^{6n_s \times 6n_s}, \quad (15)$$

with

$$W_{\text{com}} \triangleq \begin{pmatrix} [I]_{3 \times 3} & | & [0]_{3 \times 3} \\ \hat{P}_{\text{com}} & | & [I]_{3 \times 3} \end{pmatrix}^{-1} \in \mathcal{R}^{6 \times 6n_s}, \quad (16)$$

$$\begin{pmatrix} [I]_{3 \times 3} & \cdots & [I]_{3 \times 3} & | & [0]_{3 \times 3} & \cdots & [0]_{3 \times 3} \\ \hat{P}_1 & \cdots & \hat{P}_n & | & [I]_{3 \times 3} & \cdots & [I]_{3 \times 3} \end{pmatrix} \in \mathcal{R}^{6 \times 6n_s}, \quad (16)$$

and

$$W_{\text{int}} \triangleq \begin{pmatrix} S_t & R_t & \Delta_t \\ S_{\text{cop}} & T_{\text{cop}} \\ S_n & T_s \end{pmatrix} \in \mathcal{R}^{6(n_s-1) \times 6n_s}. \quad (17)$$

In the next section, we will use these models to develop controllers that can govern internal force behavior.

### III. CONTROL OF CONTACT COP'S AND INTERNAL TENSIONS/MOMENTS

We describe here a controller that governs the positions of contact centers of pressure and controls internal tensions and normal moments between contact closed loops. We integrate this controller with our previous framework involving whole-body prioritized control, unifying the control and fulfillment of constraints, tasks, and multi-contact interactions.

Let us study the multi-contact problem for  $n_s$  extremities in contact. The differential kinematics of contact points are represented as

$$\delta x_s \triangleq \begin{pmatrix} \delta x_{s(1)} \\ \vdots \\ \delta x_{s(n_s)} \end{pmatrix} = J_s \begin{pmatrix} \delta x_b \\ \delta q \end{pmatrix} \in \mathcal{R}^{6n_s}, \quad (18)$$

where  $x_{s(i)} \in \mathcal{R}^6$  is the contact CoP of the  $i^{\text{th}}$  supporting extremity,  $J_s \in \mathcal{R}^{6n_s \times (6+n)}$  is the cumulative Jacobian of all contacts,  $x_b$  and  $q$  are the robot's base and joint positions, and  $\delta$  represents the infinitesimal displacements.

In [12], we used simple rigid contact models to derive estimates of reaction forces. With the premise that stable balance is maintained and that internal forces are controlled to keep the feet at against the ground, we model contacts as rigid constraints, i.e.

$$\vartheta_s = 0, \quad \dot{\vartheta}_s = 0, \quad (19)$$

where  $\vartheta_s$  is the time derivative of  $x_s$ . These constraints allowed us to derive the simple relationship between contact forces and actuation torques [19]

$$F_r = \bar{J}_s^T U^T \Gamma - \mu_r - p_r, \quad (20)$$

where

$$\bar{J}_s \triangleq A^{-1} J_s^T (J_s A^{-1} J_s^T)^{-1} \quad (21)$$

$$\mu_r = \bar{J}_s b - \Lambda_s \dot{J}_s \begin{pmatrix} \vartheta_b \\ \dot{q} \end{pmatrix} \quad (22)$$

$$p_r = \bar{J}_s g \quad (23)$$

are the dynamically consistent generalized inverse of the Jacobian associated with contact CoP's, the Coriolis/centrifugal velocity term, and the gravity term, respectively. Additionally,

$$U = \begin{pmatrix} [0]_{n \times 6} & [I]_{n \times n} \end{pmatrix} \in \mathcal{R}^{n \times (n+6)} \quad (24)$$

is the selection matrix of actuated quantities,  $\Gamma$  is the  $n \times 1$  vector of actuation torques where  $n$  is the number of mechanical joints, and  $\mu_r$  and  $p_r$  are Coriolis/centrifugal and gravity components not shown here. In [15] we used this model to derive the following constrained whole-body equation of motion

$$A \begin{pmatrix} \dot{\vartheta}_b \\ \dot{q} \end{pmatrix} + N_s^T(b+g) + J_s^T \Lambda_s \dot{J}_s \begin{pmatrix} \vartheta_b \\ \dot{q} \end{pmatrix} = (UN_s)^T \Gamma, \quad (25)$$

where  $A$  is the mass matrix involving the unactuated base and the actuated joints,  $\vartheta_b$  is the vector of linear and angular velocities of the robot's base,

$$N_s \triangleq [I]_{6n_s \times 6n_s} - \bar{J}_s J_s \quad (26)$$

is the null space of the contact Jacobian,  $b$  and  $g$  are generalized Coriolis/centrifugal and gravity terms, and  $\Lambda_s$  is the  $6n_s \times 6n_s$  mass matrix associated with all support contacts.

To design an internal force controller, we first review our framework for whole-body multitask control. We consider a vector of task descriptors

$$x \triangleq \begin{pmatrix} x_1 \\ x_2 \\ \vdots \\ x_{n_t} \end{pmatrix} \quad (27)$$

where each  $x_k$  describes the coordinates of the  $k^{th}$  descriptor and  $n_t$  is the number of task descriptors that are used to characterize the instantaneous behavior of the robot. Prioritized task kinematics can be expressed using joint velocities alone [19], i.e.

$$\dot{x}_k = J_k \begin{pmatrix} \dot{\vartheta}_b \\ \dot{q} \end{pmatrix} = J_k \overline{UN}_s \dot{q}, \quad (28)$$

where  $\overline{UN}_s$  is the dynamically weighted generalized inverse of  $UN_s$ . The term  $J_k \overline{UN}_s$  acts as a constrained Jacobian, mapping joint velocities into task velocities. We refer to it using the symbol

$$J_k^* \triangleq J_k \overline{UN}_s. \quad (29)$$

To simultaneously control all task descriptors, we implement prioritized torque controllers under multi-contact constraints as described in [19] and characterized by the global torque vector

$$\Gamma = \sum_{k=1}^N \left( J_{k|prec(k)}^{*T} F_k \right) + N_t^{*T} \Gamma_{posture}, \quad (30)$$

where  $J_{k|prec(k)}^*$  are prioritized Jacobians,  $F_k$  are dynamically consistent control forces,  $N_t^*$  is the cumulative prioritized null space matrix associated with higher priority tasks, and  $\Gamma_{posture}$  is a postural control vector that operates in the null space of all tasks. In [19] we proposed prioritization to

unify the control of balance, constraints, tasks and postures. This unification process led to the torque control vector

$$\Gamma = J_c^{*T} F_c + J_{com|c}^{*T} F_{com} + J_{t|com|c}^{*T} F_{tasks} + J_{p|t|com|c}^{*T} F_{postures}. \quad (31)$$

where the subscript followed by  $|$  indicates prioritization and the symbols  $c$ ,  $t$ , and  $p$  denote constraints, tasks and postures. The command  $F_{com}$  is a vector of forces that directly manipulates the robot's center of mass and is used to create whole-body displacements and locomotion behaviors.

We define the space of internal forces as the projections that have no effect on the robot's motion, which can be inferred by analyzing the RHS of Equation (25). This condition leads to the following constraint:

$$(UN_s)^T \Gamma = 0 \quad (32)$$

The torques that fulfill the above constraint belong to the null space of  $(UN_s)$ , defined by the projection

$$L^* \triangleq \left( I - UN_s \overline{UN}_s \right) \in \mathcal{R}^{6 \times (n_s - 1)}, \quad (33)$$

where we use the symbol  $L^*$  to denote contact closed loops, and the superscript  $*$  to indicate that the projection operates in contact space. The torques associated with internal forces are those that do not contribute to net movement, i.e.

$$\Gamma = L^{*T} \Gamma_{int}, \quad (34)$$

where  $\Gamma_{int}$  denotes the control input to control internal forces and moments. Plugging the above torques in the RHS of (25) cancels out  $\Gamma_{int}$ .

We integrate the above structure with our prioritized controller discussed in Equation (30), leading to the unified torque structure

$$\Gamma = \sum_{k=1}^N \left( J_{k|prec(k)}^{*T} F_k \right) + N_t^{*T} \Gamma_{posture} + L^{*T} \Gamma_{int}. \quad (35)$$

Using Equations (13) and (15) we formulate the relationship between internal forces and moments with respect to contact forces as

$$F_{int} = W_{int} F_r. \quad (36)$$

The above equality implies choosing contact CoP locations to anchor the virtual linkage model. We select contact CoP locations the closest possible to the geometric center of the contact surfaces. By doing so, we avoid unwanted rotational behaviors. To ensure that these locations become the actual CoP's we neutralize CoP moments at these points, i.e.  $m_{cop} = 0$ .

The values of internal tensions and normal moments are chosen to comply with frictional constraints at the supporting surfaces (not explained here). Controlling reaction forces to remain within friction cones and frictional rotational boundaries is needed to prevent robot contact extremities from sliding and rotating with respect to the environment.

The next step consists on implementing a controller that regulates internal force behavior to desired values, i.e.

$$F_{int} \longrightarrow F_{int,ref} = \begin{pmatrix} f_{t,ref} \\ [0]_{2n_s} \\ m_{n,ref} \end{pmatrix}. \quad (37)$$

where  $f_{t,\text{ref}}$  and  $m_{n,\text{ref}}$  are desired internal force values obtained either through optimization processes as suggested before or manually chosen.

To achieve the above values, we consider using the whole-body control structure previously presented in (35). Plugging the proposed torque expression into Equation (20) and using (36) we obtain the equality

$$F_{\text{int}} = \bar{J}_{i|l}^{*T} \Gamma_{\text{int}} + F_{\text{int},\{t,p\}} - \mu_i - p_i, \quad (38)$$

where

$$\bar{J}_{i|l}^* \triangleq \left( L^* U \bar{J}_s W_{\text{int}}^T \right) \quad (39)$$

is a transformation matrix from torques to forces,

$$F_{\text{int},\{t,p\}} \triangleq W_{\text{int}} \bar{J}_s^T U^T \left[ \sum_{k=1}^N \left( J_{k|\text{prec}(k)}^{*T} F_k \right) + N_t^{*T} \Gamma_{\text{posture}} \right] \quad (40)$$

are forces induced by task and postural behavior with torques shown in Equation (35), and  $\mu_i$  and  $p_i$  are Coriolis/centrifugal and gravity terms defined as

$$\mu_i \triangleq W_{\text{int}} \mu_r, \quad (41)$$

$$p_i \triangleq W_{\text{int}} p_r. \quad (42)$$

Inverting Equation (38) we obtain the following internal force torque controller

$$\Gamma_{\text{int}} = J_{i|l}^{*T} \left( F_{\text{int,ref}} - F_{\text{int},\{t,p\}} + \mu_i + p_i \right), \quad (43)$$

where  $J_{i|l}^*$  is a left inverse of (39) and the subscript  $\{i|l\}$  denotes internal quantities operating in the space of contact closed loops. Plugging the above expression into (38) and provided that  $J_{i|l}^*$  is full row rank, we obtain the linear equality

$$F_{\text{int}} = F_{\text{int,ref}}. \quad (44)$$

To ensure that  $J_{i|l}^*$  is full row-rank,  $L^*$  needs to span all internal force and moment quantities. This applies if there are at least six independent mechanical joints separating the common ancestors between contact closed loops. A second required condition is to ensure that  $W_{\text{int}}$  defines independent internal quantities. Our definition of the virtual linkage model already ensures that  $W_{\text{int}}$  defines independent quantities.

Although, the above open loop controller will work appropriately, to achieve accurate tracking of internal forces and moments a feedback force control law involving PID (proportional-integral-derivative) feedback is preferred. Given appropriate choice of the control law, the above linear relationship will ensure convergence to the desired internal forces.

The above control structure provides a dynamically correct internal force controller that has no coupling effects on task, balance, and postural behaviors, hence enabling the efficient control of whole-body multi-contact interactions. It provides the support to simultaneously control the position of multiple contact centers of pressure and the internal tensions and normal moments acting between contact closed loops.

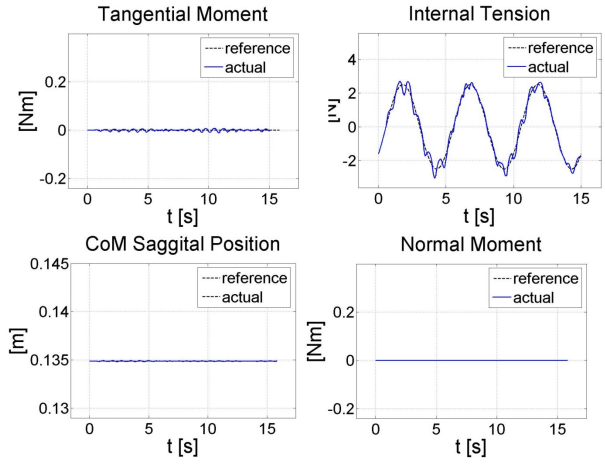
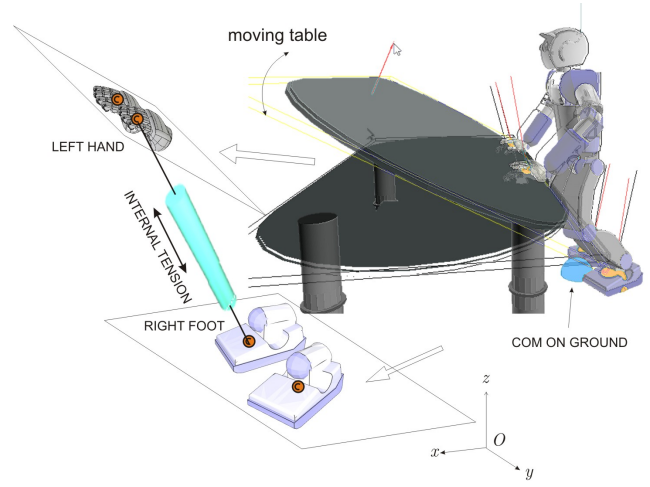


Fig. 5. Compliant stance: A four contact stance is shown here. Contact centers of pressure are controlled to stay at the center of the bodies in contact. The center of mass is controlled to remain at a fixed location. The table is actuated by an external user in random patterns to challenge the robot's contact stance. To make the skill more complicated, the internal tension between the left hand and the right foot is commanded to track a sinusoidal trajectory.

#### IV. SIMULATION RESULTS

We study an experiment on a simulated model of Asimo. Recently, we have developed a research version of Asimo that uses torque control commands [13]. The objective of this section is to demonstrate the ability to control contact CoP's, internal tensions and normal moments using the proposed methods.

A dynamic simulation environment [2] and a contact and friction simulator based on efficient propagation of forces and impacts [18] are used to simulate the execution of our methods. The whole-body controller described in (35) is implemented on a task-based software environment that enables the online creation of whole-body behaviors. Using this environment we create various behaviors involving biped and multi-contact stance as well as operational and balancing task behaviors.

In the simulation shown in Figure 5 we study a compliant multi-contact behavior that emerges from controlling contact CoP's as well as internal tensions and normal moments against contact surfaces. The robot first starts in bipedal stance and transitions to four point contact by moving hands and center of mass toward a pivoting table. This sequence

of movements is accomplished using a state machine where each state involves controlling multiple low-level task objectives. During the bipedal phase, a ZMP control strategy is implemented to ensure dynamic stability (not explained here). When transitioning to four contact stance, the robot's center of mass is controlled to track a trajectory where the accelerations are planned to fulfill contact frictional and unilateral conditions. Postural behavior is controlled by optimizing a criterion that minimizes the distance with respect to a human pre-recorded posture using a method similar to the one described in [3].

When all contacts are established, a virtual linkage model defining the internal behavior of the the four contacts (see Figure 4) is added as an additional task and the internal force controller described in Equations (35) and (43) is implemented to achieve stable compliant contact interactions. CoP points are commanded to stay at fixed locations in the middle of contact extremities. For simplicity, all tension forces as well as tangential and normal moments of Equation (37) are controlled to become zero, except for the following tracking behavior between a pair of nodes: to demonstrate force tracking at the internal level, the tension between the robot's left hand and the right foot is commanded to track the sinusoidal trajectory

$$F_{\text{int(RF-LH),ref}} = A \sin(2\pi/T), \quad (45)$$

with  $A = 4N$  and  $T = 5s$ .

A user interacts with the pivoting table by moving it up and down in random fast patterns. The robot's CoM is commanded to remain at a fixed location. Because contact CoP's are commanded to stay at the center of the extremities in contact, the hands respond compliantly to table movement, remaining flat against the moving surface.

The accompanying data graphs show tangential and normal moments, the tension between the left hand and the right foot, and the sagittal position of the CoM. The tracking error for the internal tension is small with a maximum value around 0.3 N. This error is mainly caused due to the unmodeled movement of the table. As we recall, our framework assumes that the table is static, which is implied in Equation (19). However, because the table undergoes fast accelerations the model is inaccurate. Despite this inaccuracy, the tracking behavior is still very good. In contrast, if the tabletop remains at a fixed location, the force tracking error is nearly zero (not shown here). To achieve this complex behavior we simultaneously control balance, task, and postural behaviors using the prioritize control structure shown in Equation (31) (see [19] for more details) as well as the internal force controller defined in Equation (43).

## V. CONCLUSION

Creating a virtual linkage model for humanoid robots enables the characterization of complex whole-body multi-contact interactions using simple models and the creation of new contact skills needed to operate effectively in human environments. By enabling the precise control of contact centers of pressure, we create compliant contact behaviors and by placing contact CoP's near the center of contact bodies we prevent unwanted rotations along contact edges. Characterizing the behavior of internal tensions and moments as well as the behavior of the robot's center of mass with respect to contact reaction forces we provide tools to plan maneuvering policies that satisfy all frictional constraints. Other

methods solely based on ZMP modeling disregard the local interactions between contact bodies hindering the ability to satisfy contact constraints and to create compliant contact behaviors. Our methods are dynamically correct, enabling the simultaneous control of tasks, balance, postures, and internal forces with high accuracy. We have demonstrated this ability through whole-body multi-contact examples involving upper and lower extremities in a simulated robot.

Suggestions for future work include the implementation of extreme contact behaviors such as behaviors exploiting point and edge contacts for balancing on the supports. Here, our proposed methods provide the support for the manipulation of contact centers of pressure with precision. Another key study involves using the grasp/contact matrix for planning locomotion and climbing behaviors in complex 3D terrains. Also it would be interesting to analyze contact singularities such as the case due to stretching the knees during walking behaviors.

In summary, we have presented a framework for the analysis and control of internal forces and moments acting on closed loops formed by multi-contact interactions on humanoids. We have created a new instance of the virtual linkage model to characterize the relationship between internal and CoM forces with respect to contact forces. The grasp/contact matrix associated with the virtual linkage model provides an effective tool to plan internal force and CoM behavior policies that comply with rotational and frictional contact constraints. We have analyzed the dynamics of closed loops between contacts and derived a structure to control internal forces and moments without disrupting task behavior. We have integrated this controller with our previous framework for prioritized multitasking, achieving dynamically correct control of tasks, balance, and internal forces. Finally, we have studied various simulations demonstrating the capabilities of our models and control methods in challenging multi-contact scenarios.

## ACKNOWLEDGMENTS

The financial support of Honda Motor Co. is acknowledged. Many thanks to Taizo Yoshikawa for his contributions and to Roland Philippsen and Philippe Fraise for reviewing the manuscript.

## REFERENCES

- [1] C.O. Alford and S.M. Belyeu. Coordinated control of two robot arms. In *Proceedings of the IEEE International Conference on Robotics and Automation*, pages 468–473, March 1984.
- [2] K.C. Chang and O. Khatib. Operational space dynamics: Efficient algorithms for modeling and control of branching mechanisms. In *Proceedings of the IEEE International Conference on Robotics and Automation*, April 2000.
- [3] E. Demircan, L. Sentis, V. DeSapio, and O. Khatib. Human motion reconstruction by direct control of marker trajectories. In *Advances in Robot Kinematics (ARK), 11th International Symposium*, Batz-sur-Mer, France, June 2008. Springer.
- [4] A. A. Frank. *Automatic Control Systems for Legged Locomotion Machines*. PhD thesis, University of Southern California, Los Angeles, USA, 1968.
- [5] D.T. Greenwood. *Principles of Dynamics*. Prentice-Hall, Inc., 1988.
- [6] K. Harada, S. Kajita, K. Kaneko, and H. Hirukawa. Zmp analysis for arm/leg coordination. In *Proceedings of the IEEE/RSJ International Conference on Intelligent Robots and Systems*, pages 75–81, Las Vegas, USA, October 2003.
- [7] K. Hirai, M. Hirose, Y. Haikawa, and T. Takenaka. The development of Honda humanoid robot. In *Proceedings of the IEEE International Conference on Robotics and Automation*, volume 2, pages 1321–1326, Leuven, Belgium, 1998.
- [8] R. Holmberg and O. Khatib. Development and control of a holonomic mobile robot for mobile manipulation tasks. *International Journal of Robotics Research*, 19(11):1066–1074, 2000.

- [9] S-H. Hyon, J. Hale, and G. Cheng. Full-body compliant human humanoid interaction: Balancing in the presence of unknown external forces. *IEEE Transactions on Robotics*, 23(5):884–898, October 2007.
- [10] O. Khatib. *Commande Dynamique dans l'Espace Opérationnel des Robots Manipulateurs en Présence d'Obstacles*. PhD thesis, l'École Nationale Supérieure de l'Aéronautique et de l'Espace, Toulouse, France, 1980.
- [11] O. Khatib. Object manipulation in a multi-effector robot system. In R. Bolles and B. Roth, editors, *Robotics Research 4*, pages 137–144. MIT Press, 1988.
- [12] O. Khatib, L. Sentis, and J. Park. A unified framework for whole-body humanoid robot control with multiple constraints and contacts. In *Springer Tracts in Advanced Robotics - STAR Series*, Prague, Czech Republic, March 2008.
- [13] O. Khatib, P. Thaulaud, and J. Park. Torque-position transformer for task control of position controlled robots. Patent, November 2006. Patent Number: 20060250101.
- [14] Y. Nakamura, H. Hanafusa, and T. Yoshikawa. Mechanics of coordinative manipulation by multiple robotic mechanisms. In *Proceedings of the IEEE International Conference on Robotics and Automation*, pages 991–998, April 1987.
- [15] J. Park. *Control Strategies For Robots In Contact*. PhD thesis, Stanford University, Stanford, USA, 2006.
- [16] M.H. Raibert, M. Chepponis, and H.B. Brown. Running on four legs as though they were one. *IEEE Journal of Robotics and Automation*, 2(2):70–82, June 1986.
- [17] M.H. Raibert and J.J. Craig. Hybrid position force control of manipulators. *ASME J. Dyn. Sys. Measurement Contr.*, 103(2):126–133, 1981.
- [18] D. Ruspini and O. Khatib. Collision/contact models for dynamic simulation and haptic interaction. In *The 9th International Symposium of Robotics Research (ISRR'99)*, pages 185–195, Snowbird, USA, October 1999.
- [19] L. Sentis. *Synthesis and Control of Whole-Body Behaviors in Humanoid Systems*. PhD thesis, Stanford University, Stanford, USA, 2007.
- [20] L. Sentis and O. Khatib. Task-oriented control of humanoid robots through prioritization. In *Proceeding of the IEEE/RSJ International Conference on Humanoid Robots*, Los Angeles, USA, November 2004.
- [21] L. Sentis and O. Khatib. Synthesis of whole-body behaviors through hierarchical control of behavioral primitives. *International Journal of Humanoid Robotics*, 2(4):505–518, December 2005.
- [22] M. Vukobratović and B. Borovac. Zero-moment point – thirty five years of its life. *International Journal of Humanoid Robotics*, 1(1):157–173, 2004.
- [23] D. Williams and O. Khatib. The virtual linkage: A model for internal forces in multi-grasp manipulation. In *Proceedings of the IEEE International Conference on Robotics and Automation*, pages 1025–1030, Atlanta, USA, October 1993.